Presented at the Halon Options Technical Working Conference, April 1999, Albuquerque, NM

THE ROLE OF PARTICLES IN FLAME INHIBITION BY IRON PENTACARBONYL*

Marc D. Rumminger† and Gregory T. Linteris‡
Building and Fire Research Laboratory
National Institute of Standards and Technology
Gaithersburg, MD 20899-8651, USA

INTRODUCTION

Certain metallic compounds have been found to be substantially more effective flame inhibitors than halogen-containing compounds [1-3]. In particular, iron pentacarbonyl ($Fe(CO)_5$) was found to be one of the strongest inhibitors—up to two orders of magnitude more effective than CF_3Br at reducing the burning velocity of premixed hydrocarbon-air flames [1, 4]. Although $Fe(CO)_5$ is highly toxic, understanding its inhibitory effect could lead to development of effective non-toxic agents.

Measurements of $Fe(CO)_5$-inhibited premixed flames [5-7] have shown that the inhibition varies with the $Fe(CO)_5$ concentration: at low mole fraction the burning velocity is strongly dependent on inhibitor mole fraction, while at high $Fe(CO)_5$ mole fraction the burning velocity is nearly independent of inhibitor mole fraction. A critical part of the research on $Fe(CO)_5$ is to understand iron pentacarbonyl's diminishing effectiveness at high mole fraction in order to avoid similar behavior in future fire suppressants. A plausible but unconfirmed explanation for iron pentacarbonyl's reduced effectiveness under certain conditions is that particles form, thus reducing the gas-phase mole fraction of active inhibiting species [5]. To investigate this possibility, we use laser-light scattering to measure particles in premixed flames with added $Fe(CO)_5$ and determine if the conditions of high particle concentration correspond to the regions of reduced inhibition effect. Alternatively, if there is high particle density for conditions at which $Fe(CO)_5$ has a strong inhibition effect, then the search for halon alternatives could be directed toward chemicals that produce similar condensed-phase compounds.

EXPERIMENTAL

The premixed burner system has been described previously [5]. Premixed flames are stabilized on a Mache-Hebra nozzle burner (inner diameter 1.02 ± 0.005 cm) with an air shroud flow. The burner and shroud are housed within a transparent acrylic chimney. Figure 1a shows a schematic of the flame geometry as well as the location of the scattering measurements.

---

* Official contribution of NIST, not subject to copyright in the United States.

† National Research Council / NIST postdoctoral fellow

‡ Corresponding author

Gas flows are controlled with digitally-controlled mass flow controllers. The fuel gas is methane or a mixture of carbon monoxide and hydrogen, and the oxidizer stream consists of nitrogen and oxygen. Inhibitor is added to the flame by diverting part of the nitrogen stream to a two-stage saturator, where it bubbles through liquid $Fe(CO)_5$ before returning to the main nitrogen flow.

We use laser-light scattering and extinction with phase-sensitive detection to determine particle scattering cross section and location. The apparatus is similar to those used by other researchers (e.g., [8, 9]). A simplified diagram is shown in Figure 1b; additional details about the experimental set-up and procedure can be found in Ref. [10]. The light source is a 4-W argon-ion laser, with a vertically polarized beam at 488 nm. A mechanical chopper modulates the beam at 1500 Hz and provides a reference signal for the lock-in amplifiers. A polarization-preserving single-mode optical fiber carries the light into a chemical fume hood which contains the burner, where collimating optics, a polarization rotator, mirrors and a focusing lens deliver the laser light to the test region. The light detection system consists of a reference photomultiplier tube (PMT) to measure variations in the laser power during the experiment; a photodiode to measure the transmitted light; and the 90° scattering signal optics, which include a circular aperture, collection lens, pinhole aperture, laser-line filter, polarizer and 1P28 PMT. To spatially probe the flame, a three-axis translation stage (minimum step size of 0.0016 mm) positions the burner and chimney in the stationary optical path. A personal computer controls the amplifiers and records the measurements during the experiments. In the data acquisition software, each scattering data point is normalized by the reference signal to account for variations in laser power. Typically, 100 readings are averaged over a time of about 1 second. The gas flows to the burner correspond to those of the $Fe(CO)_5$ inhibition measurements described in Refs. [5, 7].

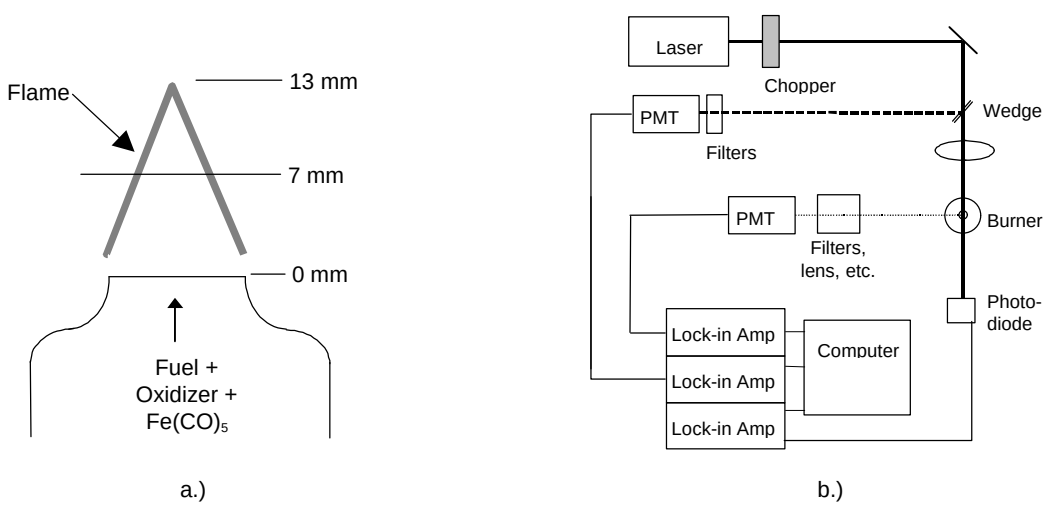

Figure 1: a.) Schematic of premixed flame, showing the dimensions of the flame. The horizontal line at 7 mm denotes the location of the measurements. The inner diameter of the burner tube is 1.02 cm. b.) Simplified schematic of experimental apparatus.

The measured quantities in the experiment are the voltage outputs of the reference, transmission, and scattered light detectors; these depend on the system geometry, optical efficiencies, detector responsivity, gas density and particle number density, and the scattering cross section of the gases or particles. To obtain the scattering cross section (Q_{vv}) of the gases or particles in the flame, a calibration is performed using a gas with known scattering cross section [8, 9]. We use room temperature ethane for calibration because of its relatively large cross section (51.6×10^{-28} cm^2 [11]).

In this study, we measure the scattering cross section (Q_{vv}), which depends on particle number density, particle material (through the refractive index), particle radius (to the sixth power), and the particle size distribution. Small changes in particle radius have a large impact on Q_{vv}; for example, increasing particle radius by 50% increases Q_{vv} by a factor of 10. Although measurement of quantities beyond Q_{vv} (such as extinction coefficient) are required to obtain detailed information about particle surface area or other chemistry-related items, Q_{vv} alone makes a clear statement about the presence of particles.

Uncertainties are reported as *expanded relative uncertainties*: $X \pm U / X \cdot 100\%$, where U is ku_c, and is determined from a combined standard uncertainty (estimated standard deviation) u_c, and a coverage factor $k = 2$ (level of confidence approximately 95%). Details about the uncertainty analysis can be found elsewhere [7, 10]. The expanded relative uncertainties for the experimentally determined quantities in this study are as follows: between 3 and 6.5% for burning velocity; between 1 and 4.5% for normalized burning velocity; 6.5% for $Fe(CO)_5$ mole fraction; 1.4% for equivalence ratio; 1.1% for oxygen mole fraction measurement; and 1.2% for hydrogen mole fraction in the reactants. The small uncertainties for these measurements are made possible through use of calibrated and computer-controlled mass flow controllers. For the scattering measurements, the combination of instability in the flame, small particle scattering cross section, large spatial gradients in the flame, and system noise cause the scattering signal to vary about a local mean value at any given location. Based on multiple measurements at each point and the calibration uncertainty, the standard deviation is no more than 10% of the mean in the particle zone and no more than 20% of the mean in the unburned reactants.

RESULTS AND DISCUSSION

METHANE FLAMES

Addition of iron pentacarbonyl to the premixed flame leads to an interesting two-zone structure for particle formation, which, unfortunately, makes extinction measurements difficult for the nozzle burner. Figure 2 provides an overview of the gross features of the particles in a premixed CH_4-air flame with 200 ppm of $Fe(CO)_5$. In Figure 2, the inner (-7 mm < r < 7 mm), lower curve was obtained using high amplifier sensitivity,

and the outer (-12 mm < r < 12 mm) curve was obtained using low sensitivity. In the central region of the figure, particles are seen to form in the main reaction zone of the flame, yielding a peak scattering signal a few times higher than that from Rayleigh scattering by the cold reactants (the signal at r = 0). These particles disappear outside the main reaction zone of the flame (4 mm < | r | < 5 mm). Far from the centerline (| r | > 10 mm), particles form with a scattering cross section almost 1000 times that of the cold reactants. Although the shroud flow around the burner probably reduces the particle formation (through dilution), the low gas velocity and low temperature in the outer annulus may cause an increase in the number of particles with a high scattering cross section. There is also the possibility that mature particles are circulating near the outer regions of the chimney. A consequence of this region of very high scattering is that it is impractical to make a measurement of the laser extinction through the region of interest (the in-flame region -7 mm < r < 7 mm at a height in the flame of 7 mm); the total extinction through the chimney is about 1%, and that is dominated by the downstream, post-combustion region of the flame which does not affect flame propagation. Because of the disparate scattering signal strengths in the two regions of the flame, the usual tomographic reconstruction techniques are impractical. Nonetheless, it is possible to accurately measure the small *scattering* signal in the flame zone by carefully positioning the flame relative to the optics, and properly adjusting the sensitivities of the lock-in amplifiers. In the absence of laser extinction data (and the resulting particle size and number density information), we can still use the scattering data to study particulate formation in the premixed flames.

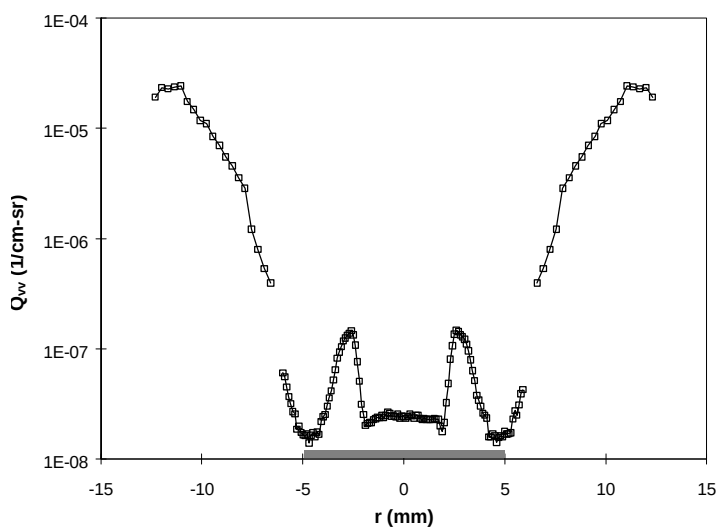

Figure 2: Scattering at 7 mm height in stoichiometric CH_4-air flame with 200 ppm of $Fe(CO)_5$. The inner curve was obtained using high amplifier sensitivity; the outer curves were obtained using low sensitivity. The grey rectangle near the x-axis marks the location of the burner exit.

In order to determine how particle formation depends on $Fe(CO)_5$ concentration, we measured radial profiles of the scattering signal for varying $Fe(CO)_5$ mole fractions (X_{in})

at a height of 7 mm above the burner rim (Figure 3). Referring to Figure 3, r = 0 corresponds to the centerline of the conical Bunsen-type flame. At this flame height (7 mm), cold reactants are in the region of $|r| < 2$ mm, the primary reaction zone of the flame extends from $|r| \sim 2$ to 3 mm, and the hot combustion products are in the region of $|r| > 3$ mm. The figure shows that at 50 ppm of $Fe(CO)_5$, Q_{vv} is only slightly higher than that of the uninhibited flame; whereas above that value, significant peaks in Q_{vv} appear in the flame zone, indicating particle formation. Note that the scattering cross section of the particles at 300 ppm is only 20 times that of room air, which implies very small diameters and/or number densities. The existence of sharp peaks in Figure 3, as opposed to a step function, may be explained as follows: in the reaction zone ($|r| \sim 2$ mm), the $Fe(CO)_5$ decomposes, resulting in supersaturated vapor of iron-containing intermediates (which are believed to be the inhibiting species). If the mole fraction of these species is high enough, nucleation and particle growth occurs. As the particles are heated by the flame ($|r| > 3$ mm), they evaporate, thus reducing their scattering cross section. Far downstream of the flame, the long residence times and cooler gases lead to formation of stable, lower vapor pressure iron oxides (seen as the very large scattering signals at $|r| > 7$ mm in Figure 2) which persist (and coat the chimney and exhaust system).

Previous experimental results [5, 6] show that the normalized burning velocity starts to level off at an $Fe(CO)_5$ mole fraction of about 100 ppm. I t has been postulated that this is due to condensation of the active iron-containing inhibiting species as they reach their saturation vapor pressure. Further, for flames at higher oxygen mole fraction (i.e. higher temperature), the leveling-off point shifts to a higher value of X_{in}. A reasonable explanation is that at higher temperature, higher concentrations of iron can remain in the gas phase before condensation occurs. Increasing the oxygen mole fraction in the air ($X_{O_2,ox}$) from 0.21 to 0.24 provides a 130 K increase in adiabatic flame temperature (see Table 1). The scattering results for higher temperature CH_4 flames ($X_{O_2,ox} = 0.24$) are shown in Figure 4. Compared to the CH_4-air results (Figure 3), the profiles have similar shape and dependence on X_{in}, but the measured Q_{vv}'s are between 2 and 4 times lower, implying fewer or smaller particles. The decreased Q_{vv} may result from the higher flame temperatures; however, the comparison is complicated by the higher burning velocity of the $X_{O_2,ox} = 0.24$ flames (see Table 1), which leads to shorter flame residence time for the particles. Alternative techniques of changing flame temperature in CH_4 flames, such as replacing some of the nitrogen with argon, also result in a simultaneous change in burning velocity. By using CO flames with added H_2, however, it is possible to change burning velocity without changing the adiabatic flame temperature, as will be described in a section below.

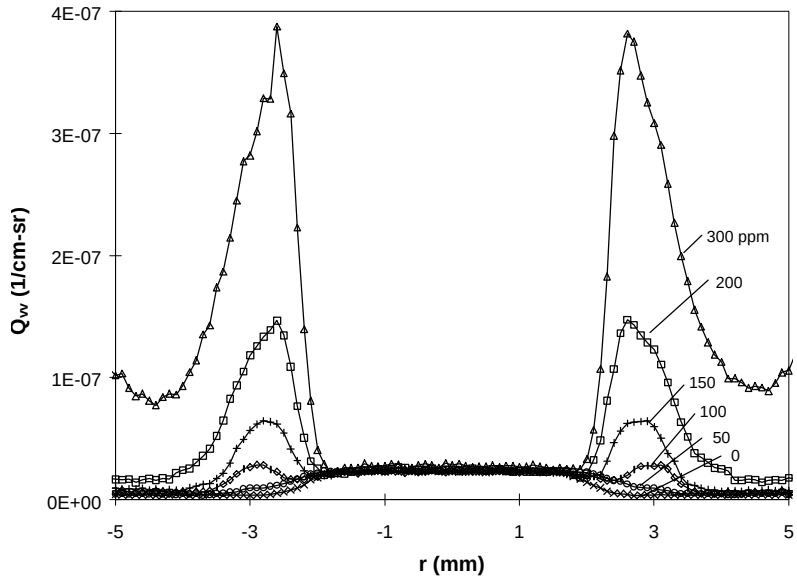

Figure 3: Measured scattering cross section through a stoichiometric CH_4-air flame 7 mm above the burner rim at various inhibitor mole fractions.

Table 1: Oxygen content of air ($X_{O_2,ox}$), mole fraction of hydrogen in reactants (X_{H_2}), measured burning velocity, and calculated maximum temperature of the stoichiometric flames used in this paper. CH_4 data from Ref. [5], CO-H_2 data from Ref. [7].

Fuel	$X_{O_2,ox}$	X_{H_2}	$v_{o,exp}$ (cm / s)	$T_{max,num}$ (K)
CH_4	0.21	0	40.6 ± 2.0	2224
	0.24	0	59.2 ± 3.0	2353
CO-H_2	0.21	0.01	39.2 ± 1.1	2376
	0.24	0.005	36.2 ± 0.9	2468
	0.24	0.01	46.2 ± 1.4	2471
	0.24	0.015	59.0 ± 2.4	2475

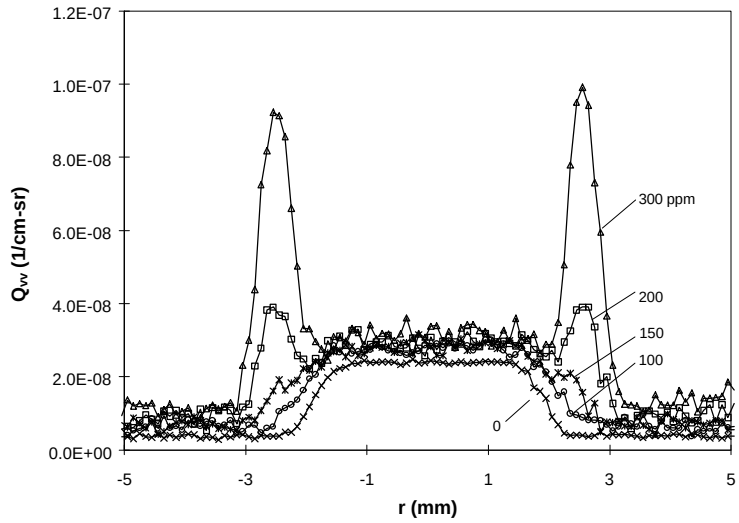

Figure 4: Scattering cross section, at a height 7 mm above the burner rim, through a stoichiometric CH_4-O_2-N_2 flame with $X_{O_2,ox}$ = 0.24 and various inhibitor mole fractions.

As stated in the Introduction, the ultimate goal of these experiments is to determine the effect of particles on flame inhibition by $Fe(CO)_5$. Therefore, we need a way to compare the data shown in Figure 3 and Figure 4 with burning velocity data of Ref. [5]. Ideally, particle surface area or molecules per particle would be used as the measure, but for the purpose of qualitative comparison, the peak Q_{vv} at each X_{in} is a reasonable choice. Note that we are limited to $X_{in} \geq 100$ ppm, because the flames with lower X_{in} show little difference in scattering compared with the uninhibited flames.

Evidence that particle formation leads to the decrease in effectiveness described previously is found in Figure 5, which shows the peak Q_{vv} along with the normalized burning velocity for various inhibitor concentrations. In regions where the normalized burning velocity depends strongly on $Fe(CO)_5$ concentration (~100 ppm), the Q_{vv} is relatively small, but as the marginal effect of the $Fe(CO)_5$ decreases to nearly zero (>200 ppm), the Q_{vv} rises sharply. By comparing the scattering and normalized burning velocity measurements at the two values of $X_{O_2,ox}$, we find additional evidence that particle formation hinders flame inhibition at high inhibitor mole fraction*: the flames with a higher inhibitor mole fraction at the leveling-off point have a smaller peak Q_{vv} at each X_{in}. Unfortunately, as mentioned above, the change of $X_{O_2,ox}$ from 0.21 to 0.24 results in increase in both flame temperature and burning velocity, and so we can not conclude which property has the primary impact on the particle formation. In the following section, these two effects will be partially decoupled.

* The difference in slope at low X_{in} is primarily a gas-phase effect [14].

There have been conflicting claims in the literature as to whether inhibition by $Fe(CO)_5$ is a gas-phase or heterogeneous effect [1, 4, 12-14]. The strong correspondence between rate of change of the normalized burning velocity and the maximum particle scattering (Figure 5) suggests that the inhibition is primarily gas-phase. If the inhibition chemistry were heterogeneous, we would expect the maximum particle scattering to be high for $Fe(CO)_5$ mole fraction below 200 ppm, and leveling-off above 200 ppm. Information about the relationship between $Fe(CO)_5$ concentration and particle surface area could help to improve understanding of the relative importance of gas-phase and heterogeneous chemistry.

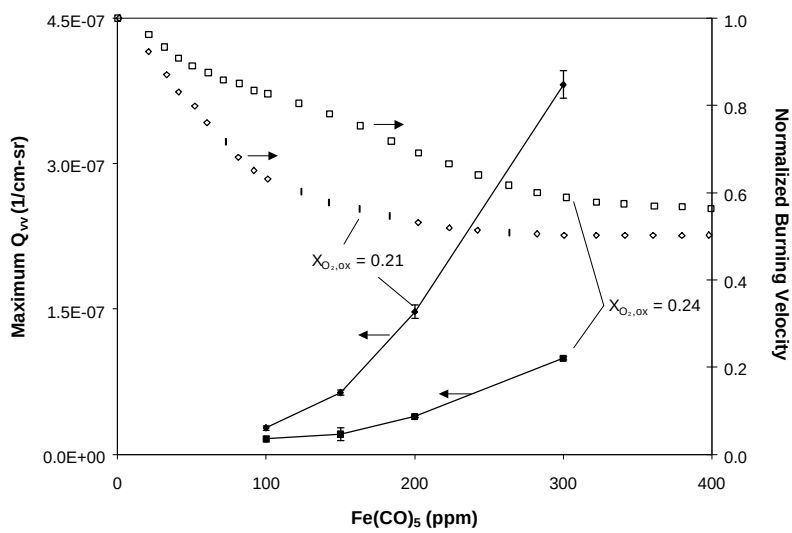

Figure 5: Normalized burning velocity and maximum Q_{vv} for ϕ=1.0 CH_4 flame with $X_{O_2,ox}$ = 0.21 and 0.24. Normalized burning velocity data from Ref. [5].

CARBON MONOXIDE FLAMES

Using CO flames with variable amounts of hydrogen in the reactants (X_{H_2}) it is possible to change the flame speed without significantly changing the flame temperature. In this study, we use stoichiometric CO flames with X_{H_2} of 0.005, 0.01, and 0.015, and elevated oxygen content relative to air ($X_{O_2,ox}$ = 0.24), giving burning velocities between 35 and 60 cm/s and adiabatic flame temperatures near 2470 K (see Table 1). Measurements of scattering cross section in each flame at various X_{in} can provide information about the relative importance of peak flame temperature and residence time.

Measured scattering cross sections for X_{H_2} = 0.005 with varying X_{in} are shown in Figure 6. Qualitatively, the results for the CO-H_2 flames are similar to those for the CH_4 flames of Figure 3 and Figure 4, in that scattering increases with increasing X_{in}, and that the particles appear and then disappear. The reasons for this may be similar to those for CH_4 flames: the newly-formed particles are small enough to evaporate as they flow

through the high-temperature region of the flame. The results for CO flames with other values of X_{H_2} (not shown) show a similar dependence of the scattering cross section on X_{in} and position.

Following the procedure used for the CH_4 flames, we correlate the scattering data with the inhibition parameters for the CO flames by plotting the peak Q_{vv} values and normalized burning velocity (from [7]) for each flame condition (Figure 7). As was seen for CH_4 flames, the peak Q_{vv} is relatively small at low X_{in} where the inhibition effect is strongest, and rises sharply as X_{in} increases. Comparing the X_{in} at which the normalized burning velocity curves level off, we see that the 0.5% H_2 curve levels off first, followed by the 1.0% H_2 and then the 1.5% H_2. Combined with the burning velocity data, the scattering results for the three values of X_{H_2} support the idea that particles reduce the inhibition effect: earlier leveling off corresponds with higher peak Q_{vv}. In other words, when more scattering occurs, the inhibition effect levels off faster.

The results in Figure 7 also show the importance of residence time for particle formation. Three flames which have roughly the same adiabatic flame temperature have very different peak scattering cross sections in the inhibited flames. This dependence on residence time can be illustrated by plotting all of the flame data together, with burning velocity (which is roughly inversely related to residence time) as the independent variable. The data, for 2 types of CH_4 flames and 4 types of CO-H_2 flames (including a stoichiometric CO-H_2-air flame with X_{H_2}=0.01), provide about 30 cm/s range of burning velocity. Figure 8 shows the maximum Q_{vv} as a function of burning velocity for the six flames considered in this paper, at X_{in} = 100 (triangles), 200 (diamonds), and 300 ppm (squares). At 100 and 200 ppm, a doubling of the burning velocity results in a halving of the maximum Q_{vv}. As the $Fe(CO)_5$ mole fraction increases, the dependence of maximum Q_{vv} on burning velocity becomes stronger, with

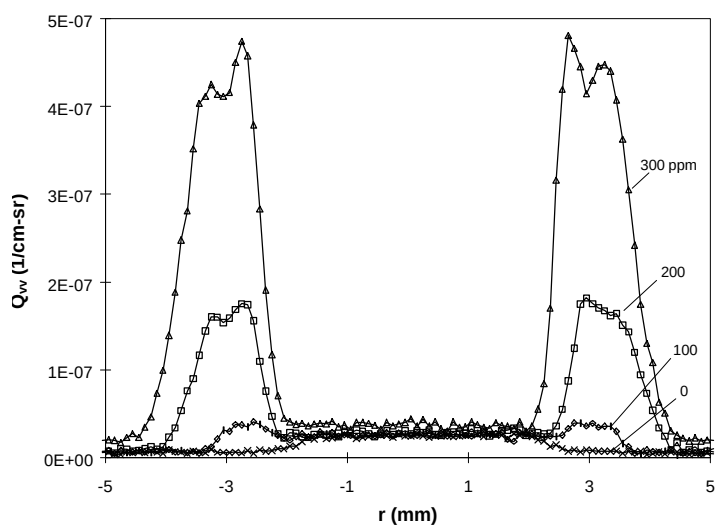

Figure 6: Scattering cross section, at a height 7 mm above the burner rim, through a stoichiometric CO-H_2–O_2-N_2 flame with X_{H_2}=0.005 and $X_{O_2,ox}$ = 0.24.

a doubling of the burning velocity from 20 to 40 cm/s leading to a four-fold decrease in the maximum Q_{vv}. A similar analysis using adiabatic flame temperature as the independent variable finds no significant relationship between maximum Q_{vv} and temperature.

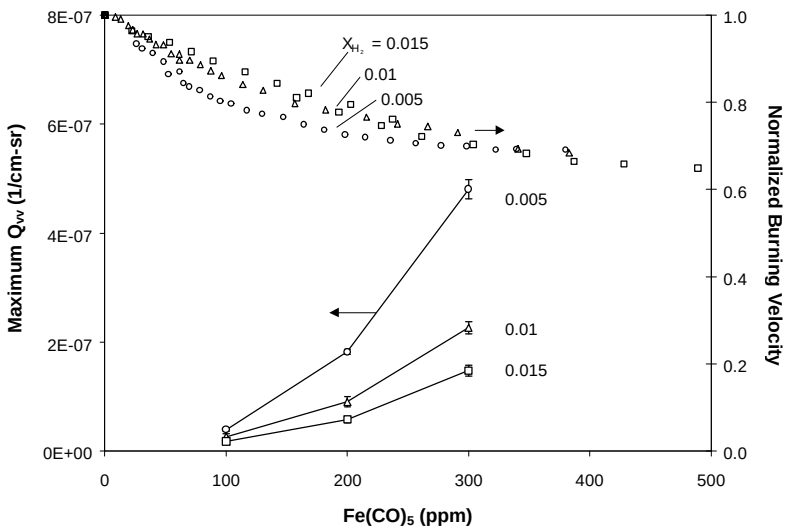

Figure 7: Maximum scattering signal and normalized burning velocity for CO-H_2 flames as $Fe(CO)_5$ concentration varies. Normalized burning velocity data from Ref. [7].

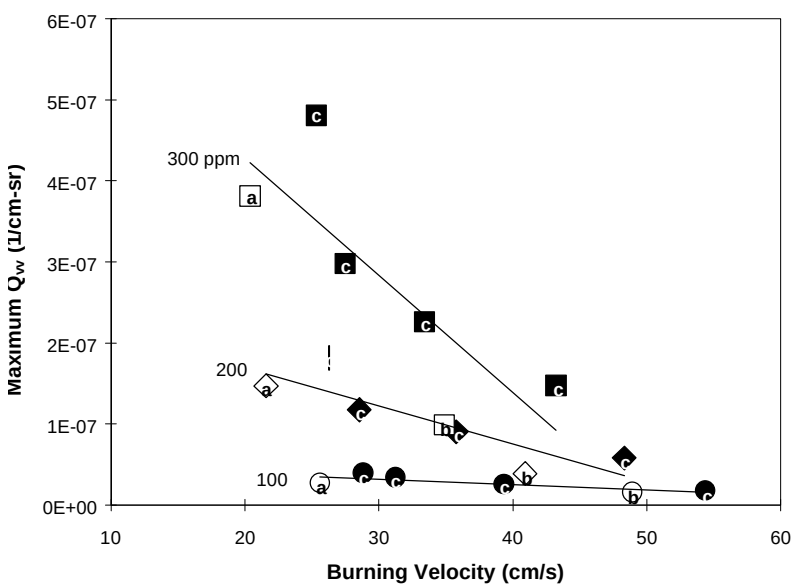

Figure 8: Maximum Q_{vv} for various X_{in} vs. burning velocity for all 6 flames. The symbol shape identifies X_{in}: 100 ppm (triangle), 200 ppm (diamond), or 300 ppm (square). The symbol color identifies the fuel: CH_4 (white) or CO (black). The letter in each symbol identifies the calculated adiabatic flame temperature: a = 2220 K, b = 2350 K, c = 2470 K. We assume that the added $Fe(CO)_5$ causes no temperature change [14]. Burning velocity data from Ref. [5] and [7].

CONCLUSION

Laser light scattering has been used to investigate particle formation in $Fe(CO)_5$-inhibited premixed flames of CH_4 and CO. Particles form early in the flame zone, reach a peak, then disappear as the temperature increases to the flame temperature; far downstream in the post-combustion gases, the peak scattering signal is several orders of magnitude larger than the peak value near the main reaction zone of the flame. The $Fe(CO)_5$ mole fraction at which the normalized burning velocity levels off corresponds to the mole fraction at which the in-flame particle formation begins to sharply increase, supporting the hypothesis that condensation reduces the inhibition, which is primarily gas-phase. Further measurements of particle size and morphology using thermophoretic sampling and electron microscopy are needed to more conclusively determine the role of particles in $Fe(CO)_5$ inhibition.

Measurements in three CO-H_2 flames with similar adiabatic flame temperatures but different burning velocities demonstrate the importance of residence time for particle formation. The highest scattering signals occur in flames with the lowest burning velocity. These results are significant since for systems with low residence time, there may not be time for condensation of iron compounds to occur during a fire-suppression event. Also, in practical systems, it may be possible to reduce the undesired loss of effectiveness due to condensation by using several compounds together, or by selecting compounds with a high vapor pressure condensed phase.

Since most fires are diffusion flames, additional particle measurements are required in counterflow diffusion flames inhibited by $Fe(CO)_5$. Previous measurements have shown large discrepancies between the measured and calculated extinction strain rate of these flames. Particle measurements may help to elucidate the reasons for the differences, and provide insights into the role of particles and active-species condensation for practical fire suppression.

The authors thank undergraduate student researcher Nikki Prive for assistance with data acquisition and uncertainty analysis programs. Discussions about particle measurement techniques with George Mulholland are gratefully acknowledged.

REFERENCES

1. Lask, G. and Wagner, H. G., "Influence of Additives on the Velocity of Laminar Flames," *Eighth Symposium (International) on Combustion*, Williams and Wilkins Co., p. 432, 1962.
2. Vanpee, M. and Shirodkar, P., "A Study of Flame Inhibition by Metal Compounds," *Seventeenth Symposium (International) on Combustion*, The Combustion Institute, p. 787, 1979.
3. Miller, D. R., Evers, R. L., and Skinner, G. B., "Effects of Various Inhibitors on

Hydrogen-Air Flame Speeds," *Combustion and Flame,* **7,** 137, 1963.

4. Bonne, U., Jost, W., and Wagner, H. G., "Iron Pentacarbonyl in Methane-Oxygen (or Air) Flames," *Fire Research Abstracts and Reviews,* **4,** 6, 1962.
5. Reinelt, D. and Linteris, G. T., "Experimental Study of the Inhibition of Premixed and Diffusion Flames by Iron Pentacarbonyl," *Twenty-Sixth Symposium (International) on Combustion*, The Combustion Institute, p. 1421, 1996.
6. Rumminger, M. D., Reinelt, D., Babushok, V., and Linteris, G. T., "Inhibition of Flames by Iron Pentacarbonyl," *Halon Options Technical Working Conference*, p. 145, 1998.
7. Rumminger, M. D. and Linteris, G. T., "Inhibition of Premixed Carbon Monoxide-Hydrogen-Oxygen-Nitrogen Flames by Iron Pentacarbonyl," submitted to *Combustion and Flame*, March 1999.
8. Santoro, R. J., Semerjian, H. G., and Dobbins, R. A., "Soot Particle Measurements in Diffusion Flames," *Combustion and Flame,* **51,** 203, 1983.
9. Charalampopoulos, T. T., Hahn, D. W., and Chang, H., "Role of Metal Additives in Light Scattering from Flame Particulates," *Applied Optics,* **31,** 6519, 1992.
10. Rumminger, M. D. and Linteris, G. T., "An Experimental Study Of The Role Of Particles In Flame Inhibition By Iron Pentacarbonyl," in preparation for submission to *Combustion and Flame*.
11. D'Alessio, A., "Laser Light Scattering and Fluorescence Diagnostics of Rich Flames Produced by Gaseous and Liquid Fuels" in *Particulate Carbon: Formation during Combustion* (Siegla, D. C. and Smith, G. W., Ed.), Plenum Press, New York, p. 207, 1981.
12. Fristrom, R. M. and Sawyer, R. F., "Flame Inhibition Chemistry", *AGARD Conference on Aircraft Fuels, Lubricants, and Fire Safety, AGARD-CP 84-71*, 1971.
13. Jensen, D. E. and Webb, B. C., "Afterburning Predictions for Metal-Modified Propellant Motor Exhausts," *AIAA Journal,* **14,** 947, 1976.
14. Rumminger, M. D., Reinelt, D., Babushok, V., and Linteris, G. T., "Numerical Study of the Inhibition of Premixed And Diffusion Flames by Iron Pentacarbonyl," *Combustion and Flame,* **116,** 207, 1999.